

# Damage Detection Through Modal Flexibility-Based Deflections: Application to a Full-Scale RC Shear Wall Building



Giacomo Bernagozzi , Said Quqa , Luca Landi ,  
and Pier Paolo Diotallevi 

**Abstract** In civil engineering structures it is highly desirable to detect the presence of damage and changes in the global structural behavior at the earliest possible stage, and, among the many existing strategies for vibration-based damage detection, modal flexibility (MF)-based approaches are promising tools. However, in most of the existing studies, the experimental validation of such approaches has been performed on small-scale laboratory structures, where damage has been artificially imposed as stiffness reductions, for example by substituting some structural elements. It is thus important to continue to test the effectiveness of such MF-based approaches on full-scale structures characterized by more realistic damaged conditions. This paper focuses on the methods for output-only damage detection and localization that are based on the estimation of structural deflections from modal flexibility, and the objective of this paper is to test the applicability of such methods for locating damage in a full-scale reinforced concrete (RC) structure that has experienced earthquake-induced damage. The considered structure is a shear wall building that can be modeled as a bending moment-deflecting cantilever structure, and was tested on the large-scale University of California, San Diego—Network for Earthquake Engineering Simulation (UCSD-NEES) shaking table. Two approaches, which are based, respectively, on the estimation of the curvature and the damage-induced rotation from the deflections, have been applied and compared on the data of the considered case study. These approaches have been applied in different scenarios characterized by different data sets and by a different number of degrees-of-freedom measured on the considered structure.

**Keywords** Structural health monitoring · Damage detection · Modal flexibility · Shear wall building · Output-only modal identification

---

G. Bernagozzi (✉) · S. Quqa · L. Landi · P. P. Diotallevi  
Department DICAM, University of Bologna, Viale Del Risorgimento 2, 40136 Bologna, Italy  
e-mail: [giacomo.bernagozzi2@unibo.it](mailto:giacomo.bernagozzi2@unibo.it)

## 1 Introduction

Structural health monitoring (SHM) strategies are becoming essential parts of the management process of civil structures and infrastructures [1]. These strategies aim to detect the presence of potential damage and changes in the structural behavior at the earliest possible stage. Such strategies also aim to support decision making in maintenance and retrofitting operations. For civil structures and infrastructures, a convenient monitoring strategy is to implement a vibration-based monitoring system and acquire the responses of the structure under ambient vibrations. Then, the acquired data can be used for identification and damage detection purposes. Referring to these two mentioned purposes, applying output-only modal identification techniques [2, 3] and modal-based damage detection techniques [1] is probably one of the most common and used approaches. These techniques are closely related since the outcomes of the former represent the starting point for the application of the latter. Moreover, the development in recent years of automated modal identification procedures [4] has contributed to close the gap between the discipline of output-only modal identification and the application of modal-based damage detection and monitoring strategies.

Among the vast class of the existing modal-based methods for damage detection, the methods based on modal flexibility and its derivatives [5–19] are promising tools. According to these approaches, the modal parameters, in terms of natural frequencies and mode shapes, are used to obtain an estimate of the static flexibility matrix of the structure. Such matrix can be considered as an experimentally-derived model of the structure, to be used for damage detection purposes. Some methods in this class are also based on an additional main step: such modal flexibility-based models are loaded by virtual loads, called inspection loads, to estimate structural deflections. Information contained in the modal flexibility matrix is thus condensed in a deflection vector, which is then used to track eventual variations that can be associated to a damaged state. Such approaches, developed in the late '90s [10], have been progressively improved and refined over the last two decades [11–19]. Some approaches based on similar damage locating concepts have been also developed to be applied from static deflections [20].

All the damage detection methods based on the estimation of modal flexibility-based deflections have some inherent common characteristics. However, each method has other specific features that depend on the type of structures for which the method has been developed. For example, such methods can be grouped into two main classes: methods developed for shear-type structures (e.g., [11–13]) and methods developed for flexure-type structures (e.g., [14–17]). Such approaches are briefly reviewed herein. In [11] an approach has been proposed for detecting and localizing damage in buildings that can be modeled as planar shear-type structures. Based on the theory presented in [11], an extension of such method has been presented in [12], where the considered structures are plan-symmetric shear-type buildings with asymmetric damage. The problem of detecting damage in shear-type buildings using modal flexibility-based deflections is also addressed in [13], where different

strategies have been proposed for performing the calculations with minimal or no a priori information about the structural masses, even in the case in which the masses are varied before and after damage. In [14] the displacements and the curvatures of modal flexibility-based deflections have been analyzed for damage localization on a steel grid laboratory model. In [15] the concept of the Positive Bending Inspection Load (PBIL) has been introduced, and a method has been presented for damage localization in simply supported and continuous beams. In [16] the damage localization for beam-like structures is carried out using the normalized curvature of the uniform load surface evaluated from modal flexibility. This approach has been verified through numerical simulations performed for a cantilever beam and for a simply supported beam, by considering measured degrees-of-freedom (DOFs) at the same spacing. In [17] a method is presented for damage localization in cantilever beam-type structures. The experimental verification of this approach has been performed using a laboratory 10-story frame model with constant interstory heights and by measuring the structural responses at all stories.

It is important to underline that in most of the existing studies related to the application of methods based on modal flexibility-based deflections, the experimental validation has been performed on small-scale laboratory structures. Studies where these approaches have been validated using full-scale structures exist, but the number of such studies with full-scale validations is quite small compared to the studies that considered small-scale laboratory structures. For example, in [18] modal flexibility and modal flexibility-based deflections have been used for condition assessment in real-life bridges. As another example, in [19] the approach presented in [11] has been validated on a full-scale shear building, where damage has been imposed by replacing a spring member with other members having reduced stiffness. Based on these premises, it is thus evident that is important and of interest to continue to test the effectiveness of the methods based on modal flexibility-based deflections on full-scale structures.

The objective of this paper is to test the applicability of the damage localization methods based on the estimation of modal flexibility-based deflections on a full-scale reinforced concrete (RC) structure that has experienced earthquake-induced damage. The considered structure is a shear wall building that can be modeled as a bending moment-deflecting cantilever structure. In particular, two approaches for damage localization have been applied and compared on the data of the considered case study. These approaches have been applied by considering different scenarios characterized by different data sets and by a different number of degrees-of-freedom measured on the considered structure.

## 2 Damage Detection Through Modal Flexibility-Based Deflections in Bending Moment-Deflecting Cantilever Structures

The modal flexibility matrix of a generic structure can be defined as an estimate of the static flexibility matrix of the considered structure obtained from a vibration test, and specifically from the extracted modal parameters. When dealing with input-output tests, such matrix can be directly extracted from the data if for at least one degree-of-freedom both the input force and the output response are measured. This requirement guarantees that mass-normalized mode shapes can be estimated. When dealing with output-only tests, the modal flexibility matrix is not readily available from the data [8]. However, solutions exist to circumvent the problem and to obtain the mass-normalizing constants required to estimate the modal flexibility from output-only data. One can use mode shape scaling techniques, which generally need the execution of additional tests with some imposed structural modifications [3]. As a second option, one can use an a priori estimate of the system mass matrix [11, 12] or can use the mass matrix of the structure derived from a FEM model [3]. As a third option, one can try to extract from the output-only data unscaled matrices that are proportional to the mass and flexibility matrices of the structure [6, 8, 9, 13, 21], indicated, respectively, as proportional mass matrices (PMMs) and proportional flexibility matrices (PFMs). When considering this last case and using the estimated proportional flexibility matrices for damage detection purposes, it is important to consider PFMs in the baseline and in the potentially damaged states that are properly scaled. Usually, this condition is guaranteed if the masses are unchanged in the different considered states of the structure and if the same PMM is used to normalize the mode shapes in the baseline and in the potentially damaged states [6, 13]. Estimating modal flexibility matrices from vibration data is in general an operation that can be performed also in the case in which not all the DOFs of the structure are measured, as shown in [7] for the input-output case or in [6, 9] for the output-only case.

The modal flexibility matrix of a generic MDOF classically-damped structure can be obtained using the following equation [7–9]:

$$\mathbf{F}_{r \ n \times \ n} = \sum_{i=1}^r \frac{1}{(s_i \omega_i)^2} \boldsymbol{\psi}_i \boldsymbol{\psi}_i^T \quad (1)$$

where  $n$  is the number of the DOFs measured on the structure,  $r$  is the number of the modes included in the calculations,  $\boldsymbol{\psi}_i$  is the  $i$ th real arbitrarily-scaled mode shape vector (with dimensions  $n \times 1$ ),  $\omega_i$  is the  $i$ th natural circular frequency, and  $s_i$  is the mass normalization factor for the  $i$ th mode.

After having estimated the modal flexibility matrices, a convenient approach to tackle the damage detection problem is to calculate the modal flexibility-based deflections. Such deflections can be determined by applying some inspection loads to the

flexibility-based experimentally-identified model of the structure, as follows

$$\mathbf{v} = \mathbf{F}_r \mathbf{p} \quad (2)$$

where  $\mathbf{v}_{n \times 1}$  is the modal flexibility-based deflection and  $\mathbf{p}_{n \times 1}$  is the inspection load. When considering bending moment-deflecting beam-like structures, a Positive Bending Inspection Load (PBIL) is usually selected as the inspection load. The PBIL is a load that generates positive bending moments in the inspection region of the structure and no inflection points in the deflection within that region [15].

After having estimated the modal flexibility-based deflections, different features computed from these deflections can be used for damage detection. Some examples of existing approaches are mentioned: in [14] the displacement and the curvature are used; in [15] the additional deflection measured from the chord that connects two DOFs is evaluated; in [16] the normalized curvature of a uniform load surface is used; in [17] the interstory deflection is evaluated. The works [15–17] also show the relationship that exists between damage in beam-like structures (e.g., a localized stiffness reduction) and the damage-induced deflection, i.e., the difference between the deflections in the damaged and undamaged states. These mentioned approaches represented the starting point for the development of the damage detection approaches that in this paper are applied to the data of the considered case study, which, as already mentioned, is a full-scale reinforced concrete structure that has experienced earthquake-induced damage. This structure, described in Sect. 3, can be modeled as a bending moment-deflecting cantilever structure, and thus the analytical formulation presented in the remaining part of this section was developed by considering these types of structures. It is also important to mention that the approaches and analyses presented in this paper focus on planar structures, whose structural behavior is analyzed in one direction (Fig. 1).

For a cantilever structure, a convenient inspection load to be adopted for evaluating the modal flexibility-based deflections is a uniform load with unitary values at all the DOFs—i.e.,  $\mathbf{p} = \{1 \ 1 \ \dots \ 1\}^T$ . This load is a PBIL load for a cantilever structure, as shown in [15]. Starting from the displacements of the calculated deflection, the rotations and the curvatures can be estimated using the finite difference method, as a numerical derivation technique.

The rotation of a portion of the structure located between two measured DOFs—i.e., the  $(j + 1)$ th and the  $j$ th DOFs—can be estimated as follows:

$$\varphi_{(j+1,j)} = \frac{v_{j+1} - v_j}{h_{j+1} - h_j} \quad (3)$$

where  $h_j$  is the height of the  $j$ th DOF evaluated with respect to the base of the cantilever structure. If the measured DOFs are located at a constant spacing equal to  $\Delta h$ , Eq. (3) is simplified as follows:

$$\varphi_{(j+1,j)} = \frac{v_{j+1} - v_j}{\Delta h} \quad (4)$$

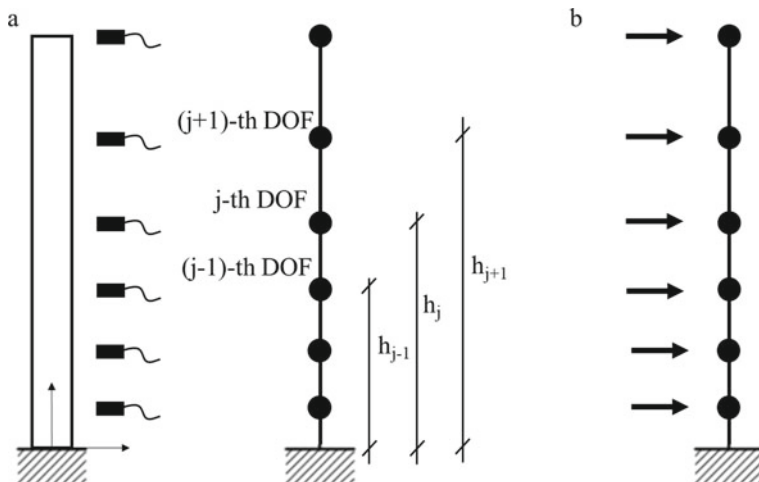


**Fig. 1** Bending moment-deflecting cantilever structure: **a** structural model with a generic sensor layout; **b** applied inspection load

The curvature at the  $j$ th measured DOF of the modal flexibility-based deflections can be estimated as follows:

$$\chi_j = \frac{\frac{v_{j+1}-v_j}{h_{j+1}-h_j} - \frac{v_j-v_{j-1}}{h_j-h_{j-1}}}{\frac{h_{j+1}-h_{j-1}}{2}} \quad (5)$$

Equation (5) is valid for measured DOFs that are unevenly distributed along the height of the structure. Such equation was obtained by adapting the formulation presented in [22], for evaluating the curvature of mode shapes and operational deflection shapes, to the case of the modal flexibility-based deflections. If the measured DOFs are located at a constant spacing equal to  $\Delta h$ , Eq. (5) is simplified as follows:

$$\chi_j = \frac{v_{j+1} - 2v_j + v_{j-1}}{\Delta h^2} \quad (6)$$

In this paper, the quantities presented in Eqs. (3) and (5) are used for damage localization purposes. Of course, uncertainties are always present on quantities extracted from real noisy vibration data. Thus, statistical approaches based on outlier analysis [1] are introduced in the damage localization process. To implement these statistical approaches, it is required that the calculations related to the baseline structure are repeated using different portions of the training data set. This is done to estimate the degree of variability that affects the quantities related to the baseline structure.

Two different damage localization strategies were developed and then applied to the data of the considered case study.

According to the first strategy, the values of the curvature are monitored, and it is of interest to see if the values of the curvature in the potentially damaged state deviate from the values of the curvature related to the baseline structure. This strategy is implemented through the calculation of the following index, which is herein defined as z-index based on curvature

$$z_{\chi,j} = \frac{\chi_{I,j} - \bar{\chi}_{B,j}}{s(\chi_{B,j})} \tag{7}$$

Equation (7) can be evaluated for each *j*th measured DOF with  $j = 1 \dots n - 1$ , where  $j = 1$  is the first measured DOF at the bottom of the structure. In Eq. (7)  $\chi_{I,j}$  is the curvature related to the structure in the inspection stage, and  $\bar{\chi}_{B,j}$  and  $s(\chi_{B,j})$  are the sample mean and the sample standard deviation of the curvature  $\chi_{B,j,i}$  evaluated from the training data set (for  $i = 1 \dots q$  where  $q$  is the total number of damage-sensitive features extracted from the training data set).

In the second strategy for damage localization, the concept of the damage-induced rotation is introduced, which is the difference between the rotation in the inspection stage and the rotation related to the baseline state. In particular, the second strategy is based on tracking eventual variations in the damage-induced rotation along the height of the cantilever structure. This strategy is implemented through the calculation of the following index, which is herein defined as z-index based on a damage-induced rotation

$$z_{\varphi,j} = \frac{\Delta\bar{\varphi}_{(j+1,j)} - \Delta\bar{\varphi}_{(j,j-1)}}{s(\Delta\varphi_{(j,j-1)})} \tag{8}$$

Equation (8) can be evaluated for each *j*th measured DOF with  $j = 1 \dots n - 1$ , and in Eq. (8) the damage-induced rotations of adjacent portions of the structure are considered. The terms  $\Delta\bar{\varphi}_{(j+1,j)}$  and  $\Delta\bar{\varphi}_{(j,j-1)}$  are defined as follows:

$$\Delta\bar{\varphi}_{(j+1,j)} = \varphi_{I,(j+1,j)} - \bar{\varphi}_{B,(j+1,j)} \tag{9}$$

$$\Delta\bar{\varphi}_{(j,j-1)} = \varphi_{I,(j,j-1)} - \bar{\varphi}_{B,(j,j-1)} \tag{10}$$

where the symbol  $\Delta$  indicates that, for the considered quantity, the difference between the inspection stage and the baseline state is performed. As already shown for Eq. (7), the operators  $\bar{\cdot}$  and  $s(\cdot)$  present in Eqs. (8), (9) and (10) calculate the sample mean and the sample standard deviation, respectively, and are applied on quantities related to the baseline state.

Both in the first and in the second strategy, the z index has to be compared to a threshold value  $z^{TH}$  in order to understand if the structure has undergone structural modifications which can be associated with a damaged state and to identify the locations of the damage. For the *j*th measured DOF, the structure in the inspection stage is considered as unaltered with respect to the baseline structure if  $z_{\chi,j} \leq z^{TH}$

(first strategy) and  $z_{\varphi,j} \leq z^{TH}$  (second strategy). For the  $j$ th measured DOF, it is recognized that the structure in the inspection stage deviates from the baseline state if  $z_{\chi,j} > z^{TH}$  (first strategy) and  $z_{\varphi,j} > z^{TH}$  (second strategy). Assuming that the features extracted from the training data set have a normal distribution, as it is also done in [12, 13] where similar statistical tests have been performed, the value of the threshold is assumed as equal to  $z^{TH} = 3$ .

As shown in Eqs. (7) and (8), the quantities considered in the two indices for the damage localization statistical tests are different, and thus different outcomes are in general obtained using the two strategies. However, it is also important to underline that the two strategies have an inherent similarity, which is shown using the following analytical formulation.

The numerator in the expression of the  $z$  index based on damage-induced rotation—i.e., the numerator of the second term in Eq. (8)—is considered, and such term is divided by the term  $\frac{h_{j+1}-h_{j-1}}{2}$ , as shown in Eq. (11a). Then, Eqs. (9) and (10) are substituted into Eq. (11a), and the terms of the derived Eq. (11b) are rearranged as shown in Eqs. (11c) and (11d). Through the definitions of the rotation and the curvature expressed by Eqs. (3) and (5), it can be recognized that Eq. (11d) can be finally reformulated as the difference between the curvature in the inspection stage and the sample mean of the curvature related to the baseline structure. This difference is the numerator in the expression of the  $z$  index based on curvature—i.e., the numerator of the second term in Eq. (7).

$$\frac{\Delta\bar{\varphi}_{(j+1,j)} - \Delta\bar{\varphi}_{(j,j-1)}}{\frac{h_{j+1}-h_{j-1}}{2}} = \quad (11a)$$

$$= \frac{\varphi_{I,(j+1,j)} - \bar{\varphi}_{B,(j+1,j)} - (\varphi_{I,(j,j-1)} - \bar{\varphi}_{B,(j,j-1)})}{\frac{h_{j+1}-h_{j-1}}{2}} = \quad (11b)$$

$$= \frac{\varphi_{I,(j+1,j)} - \varphi_{I,(j,j-1)} - (\bar{\varphi}_{B,(j+1,j)} - \bar{\varphi}_{B,(j,j-1)})}{\frac{h_{j+1}-h_{j-1}}{2}} = \quad (11c)$$

$$= \frac{\varphi_{I,(j+1,j)} - \varphi_{I,(j,j-1)}}{\frac{h_{j+1}-h_{j-1}}{2}} - \frac{\bar{\varphi}_{B,(j+1,j)} - \bar{\varphi}_{B,(j,j-1)}}{\frac{h_{j+1}-h_{j-1}}{2}} = \chi_{I,j} - \bar{\chi}_{B,j} \quad (11d)$$

### 3 Application to a Full-Scale RC Shear Wall Building

The damage localization approaches described in the previous section were applied on the data of experimental tests that were performed on a full-scale reinforced concrete structure that has experienced earthquake-induced damage. These experimental tests were performed between September 2005 and May 2006 at the Englekirk Structural Research Center, using the University of California–San Diego Network



for Earthquake Engineering Simulation (UCSD-NEES) large outdoor unidirectional shake table. The data of this experimental program were retrieved from [23]. The tested structure is 63 ft (i.e., 19.2 m) high and is formed by shear walls. Such structure can be considered as a portion of a 7-story residential building that has structural walls as the lateral force-resisting system (Fig. 2). The structure has one main longitudinal web wall, which is 12 ft (i.e., 3.66 m) long, and two transverse walls, which provided lateral and torsional stability during the tests. A 12 ft by 26 ft–8 in. (i.e., 3.66 m by 8.13 m) slab is present at each floor level, and such slab is supported by the walls and by some gravity columns. The structure was positioned on the shake table with the main longitudinal wall aligned to the direction of the base excitation (i.e., east–west direction) and was instrumented with a dense array of sensors, including accelerometers for measuring the vibration responses. During the experimental program, some historical earthquake records were applied at the base of the structure, which induced progressively increasing levels of damage. After each strong motion test, low-amplitude white noise base excitation tests and ambient vibration tests were performed for damage characterization purposes. More detailed information about the structure and the performed vibration tests can be found in [24–26].

For the analyses of the present paper, only a subset of the vibration tests, sensor data, and structural configurations of the whole experimental program performed on the UCSD-NEES shake table has been considered. Referring to the structural

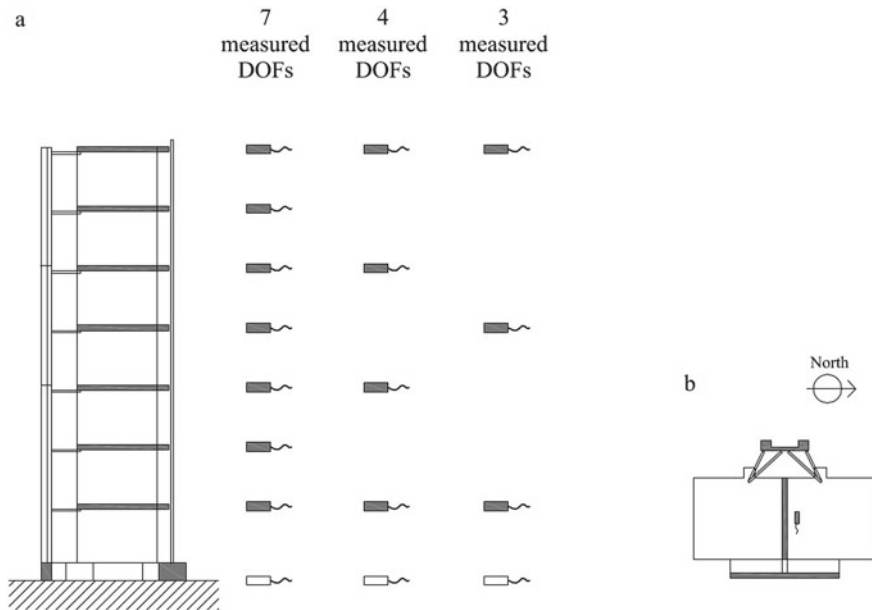


**Fig. 2** Schematic drawing of the geometry of the structure with indications of the measured DOFs (geometry retrieved from [23, 24]): **a** elevation—south face; **b** floor plan view

configurations, in this paper the following configurations (tested progressively) and damaged states were considered: S0 which is the baseline configuration; S1 which is the damaged state that resulted from the application of the longitudinal component of the San Fernando earthquake measured in 1971 at the Van Nuys station (EQ1); S2 which is the damaged state obtained by subsequently subjecting the structure to the transversal component of the above-mentioned San Fernando earthquake (EQ2); S3.1 which is the damaged state generated by subsequently applying at the base of the structure the longitudinal component of the Northridge earthquake measured in 1994 at the Oxnard Boulevard station in Woodland Hill (EQ3) [25, 26]. The other damaged states shown in [25, 26] (i.e., S3.2 and S4) were not considered in the analyses of the present paper. As observed in [25, 26], after state S3.1 some braces present in the structure were strengthened and stiffened. Thus, for the analyses of the present paper it was considered appropriate to start focusing on the configurations tested before the strengthening intervention, and the states S3.2 and S4 may be considered in future developments of the work.

Referring to the type of vibration tests, the analyses of the present paper focus on the data of the tests performed, for each configuration and damaged state, by applying at the base of the structure a 0.03 g root mean square (RMS) white noise excitation with a duration of 8 min. Referring to the sensor data, this paper focuses on the analysis of the data collected using the accelerometers that were positioned at the different floor levels near the main longitudinal wall and oriented in the direction of the base excitation (Fig. 2b). These data were used to perform a planar analysis of the considered structure. In particular, three different scenarios characterized by different data sets and by a different number of degrees-of-freedom measured on the structure were considered in the analyses. As shown in Fig. 2a, a first analysis was done by considering the data collected at 7 DOFs—i.e., the data measured at each floor level from 1 to 7. In a second analysis, 4 measured DOFs were considered—i.e., the DOFs located at floor levels 1,3,5,7. Finally, a third analysis was performed by considering the data measured at 3 DOFs—i.e., the data measured at floor levels 1,4,7. In all three different considered scenarios, the accelerations at the base of the structure (i.e., floor level 0) were also included in the calculations, as discussed later in this section. All the measurements used for the analyses have a sampling frequency ( $f_s$ ) equal to 240 Hz.

Before proceeding with the presentation of the performed analyses and related results, it is important to describe the damage that was observed in the structure during the experimental tests. This in fact represents the expected outcome of the applied damage localization approaches. As described in detail in [25], damage in the structure was observed visually (through pictures and video recordings), and it was also deduced from strain sensors. As stated in [25], the actual damage observed in the structure is characterized by a concentration of damage at the bottom two stories of the longitudinal web wall. This damage scenario matches the outcome of the vibration-based strategy for damage detection, localization, and quantification that was applied in [25] starting from the acceleration measurements—i.e., a sensitivity-based finite element (FE) model updating strategy. Through the analysis of the strain data and using the FE model updating damage detection method, in [25] it was also

observed that the extent of damage increases as the structure is exposed to stronger earthquake excitations.

As a first step in the analyses, the absolute accelerations related to each measured DOF were converted into relative accelerations, by subtracting from the absolute accelerations the accelerations measured at the base of the structure. Then, an output-only modal identification algorithm—i.e., the Natural Excitation technique (NExT) [27] combined with the Eigensystem Realization Algorithm (ERA) [28]—was used to estimate the modal parameters of the structure. In particular, the training data set was divided into 8 different portions (with a duration of 1 min each), and each different portion was used to estimate the modal parameters. This was done for estimating the degree of variability that affects the quantities related to the baseline state, which is a fundamental step required for applying the subsequent statistical approaches for damage localization. It is important to point out that considering only 8 portions of the signals is not the optimal number of samples for the assumed model of having baseline DSFs with a normal distribution. However, given the duration of the training data set related to the 0.03 g RMS white noise base excitation tests, this choice was done to manage the trade off between the considered number of the measurement portions and the time length of such signals. It is worth noting that an attempt was also made to perform similar operations for the training data set by considering the ambient vibration tests, which have a duration of 3 min. In such case, however, due to a shorter measurement duration, it was much harder to estimate adequately the degree of variability on the quantities related to the baseline state. The data of such ambient vibration tests were thus not considered in the analyses of the present paper, and they may be considered in future developments of the work focused on performing the calculations with small training data sets.

The NExT-ERA identification algorithm was also applied for the other considered states of the structure. In general, starting from the data of the considered measured DOFs (Fig. 2) it was possible, for each structural state, to identify the first three longitudinal modes of the structure in the direction of the applied white noise base excitation. These first three longitudinal modes were then used for the damage detection analyses of the present paper, which is the same number of modes that was considered for detecting damage in the analyses presented in [25]. The natural frequencies identified for the different states of the structure are provided in Table 1, which also shows the percent variations evaluated with respect to the frequencies

**Table 1** Identified natural frequencies of the structure in the different states

State	Natural frequency $f_i$ (Hz) (% variation w.r.t. baseline state $S_0$ )		
	1st mode	2nd mode	3rd mode
$S_0^a$	1.69	11.53	24.81
S1	1.53 (−9.8)	11.32 (−1.9)	24.67 (−0.6)
S2	1.23 (−27.3)	10.56 (−8.4)	23.41 (−5.6)
S3.1	1.11 (−34.4)	7.88 (−31.6)	19.72 (−20.5)

<sup>a</sup>Mean values of natural frequencies

of the baseline state  $S_0$ . From Table 1, it can be observed, as expected, that the frequencies related to the damaged states are lower than the frequencies of the baseline structure. Moreover, the frequencies progressively decrease when considering structural states characterized by more severe damage.

The identified modal parameters were used to assemble the modal flexibility matrices of the structure in the different states using Eq. (1). In particular, the mass matrix of the structure was estimated a priori using the available information about the structure and used for obtaining the mass normalization factors for the different modes. When evaluating the mass matrix of the considered beam-like cantilever structure, the following two simplified assumptions were made: it was assumed to neglect the rotational inertia of the considered DOFs, and it was assumed that the mass is uniformly distributed along the height of the structure. Moreover, it was not of interest to estimate the true scaled values of the masses, but only values that are proportional to the corresponding true scaled values. This resulted in estimating diagonal mass matrices whose components are proportional to the structural masses that refer to the measured DOFs, considered in the different scenarios. The use of proportional mass matrices led to the estimation of proportional flexibility matrices, which were then used to estimate the modal flexibility-based deflections. This was done according to Eq. (2), and a uniform load with unitary values at all the measured DOFs was considered as the inspection load. As an example, the modal flexibility-based deflections of the structure in the different states evaluated for the scenario with 7 measured DOFs are reported in Fig. 3. In particular, the displacements, the rotations, and the curvatures of the deflections are reported in Fig. 3a, b, and c, respectively.

By analyzing Fig. 3, it can be observed that the experimentally-derived deflections are in general in agreement with the deflections that one expects to have from a theoretical model of a bending moment-deflecting cantilever structure. There are, however, some discrepancies between the former and the latter, especially referring to the curvatures. The values of the curvature shown in Fig. 3c tend to increase from the upper to the lower DOFs, as expected. However, it can be observed that there is an inversion in the curvature at DOF number 6, while the curvature goes to zero at DOF number 3, creating an irregular trend. On one side, these effects and observed trends could be due to inevitable uncertainties related to the process of estimating the curvature of experimental deflections using the approximated finite difference method. On the other side, it is evident that idealizing and modeling the considered structure as a bending moment-deflecting cantilever structure (Fig. 1) is probably one of the simplest approaches, which leads to inevitable approximations. Using more complex numerical FE models for damage detection purposes is, however, beyond the scope of the present research, which has been developed based on the following general idea that is behind all modal flexibility-based approaches for damage detection—i.e., it is attempted to extract an experimental model of the structure directly from the measured data, without the actual need of assembling a numerical FE model.

From Fig. 3a, it can also be observed that the values of the displacements increase when considering, in the order, the baseline state and the states  $S_1$ ,  $S_2$ , and  $S_{3.1}$ . This is a clear indication that structural modifications have occurred between the

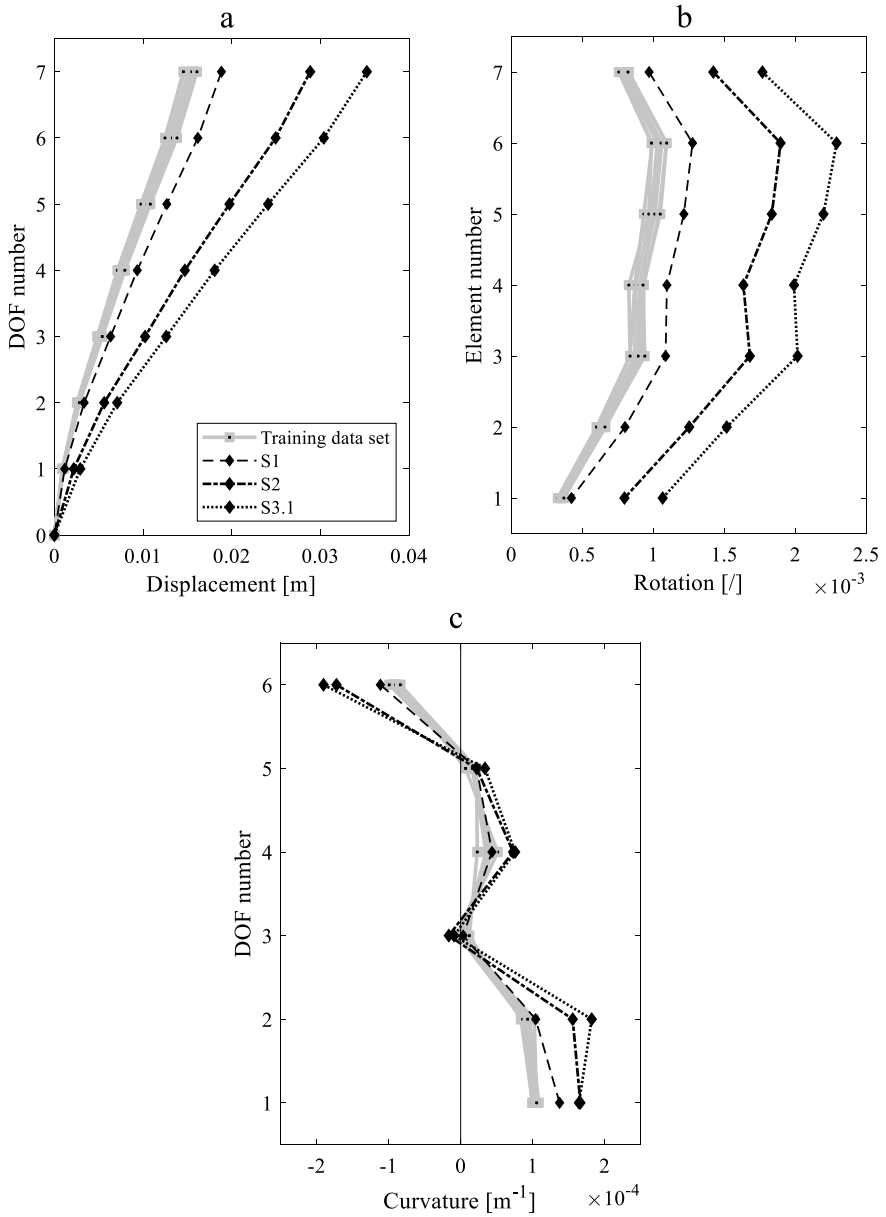


**Fig. 3** Modal flexibility-based deflections of the structure in the different states obtained for the scenario with 7 measured DOFs: **a** displacements; **b** rotations; **c** curvatures

different states. These deflections in fact have been evaluated for the same load, and the observed increases in the values of the displacements show evidence that the considered structural states are characterized by increasing values of the flexibility (i.e., decreasing values of the stiffness).

The results of the damage localization are reported in Fig. 4, where Fig. 4a, c, and e show the results obtained using the  $z$  index based on curvature (Eq. 7), while Fig. 4b, d, and f present the results obtained through the  $z$  index based on damage-induced rotation (Eq. 8). In this figure, the application of the approaches based on the  $z$  index is presented for the three considered scenarios: Fig. 4a, b refer to the scenario with 7 measured DOFs; Fig. 4c, d show the results obtained in the scenario with 4 measured DOFs; Fig. 4e, f refer to the scenario with 3 measured DOFs. As shown in the figure, both two  $z$  indices were evaluated for  $j = 1 \dots n - 1$ , where  $n$  is the number of the measured DOFs.

As evident in Fig. 4a, b for the scenario with 7 measured DOFs, both two  $z$  indices provide localization of the damage that is consistent with the actual damage observed in the structure, which, as mentioned in [25], is concentrated at the bottom two stories of the structure. In particular, through the adopted  $z$  indices it is possible to detect the DOFs of the structure that have been affected by the damage. It can be observed from Fig. 4b that the values of the  $z$  index based on damage-induced rotation at the upper DOFs are lower than the corresponding values at the bottom of the structure, with values of  $z$  index at the DOF number 3, 4, 5 and 6 that are all below the threshold. This is in general true also for Fig. 4a ( $z$  index based on curvature), where, however, it can be observed that for some upper DOFs the  $z$  index is slightly higher than the threshold (such cases shown in Fig. 4a can be considered as false positives). The results obtained for the scenarios with 4 measured DOFs and 3 measured DOFs also show a concentration of damage for the DOFs at the bottom of the structure, and if one compares the results obtained using the two  $z$  indices, this effect is more evident in the results obtained using the  $z$  index based on damage-induced rotation (Fig. 4d, f).

The considered  $z$  indices were developed for performing statistical tests for damage detection and localization, and they were not explicitly derived for damage quantification purposes. However, the results presented in Fig. 4 clearly show that the values of both two  $z$  indices tend to increase for states that have undergone a higher number of earthquake excitations (i.e., considering in the order the states S1, S2, and S3.1), and this is consistent with what has been observed in [25]. In this perspective of considering the  $z$  indices also for obtaining an indication of the extent of damage, some important differences can be observed in the results obtained using the two  $z$  indices. Using the  $z$  index based on curvature in the scenario with 4 measured DOFs (Fig. 4c) the maximum value of the  $z$  index is at the DOF number 3, and this is especially evident for state S3.1. This observed trend with a maximum for an intermediate DOF of the structure seems to be not consistent with the results obtained in this paper using the same  $z$  index in the other scenarios (Fig. 4a, e) and not consistent with the concentration of damage at the bottom of the structure observed in the experimental tests [25]. This inconsistency found in the results obtained using the  $z$  index based on curvature, is, on the contrary, not present in the results obtained using the  $z$  index

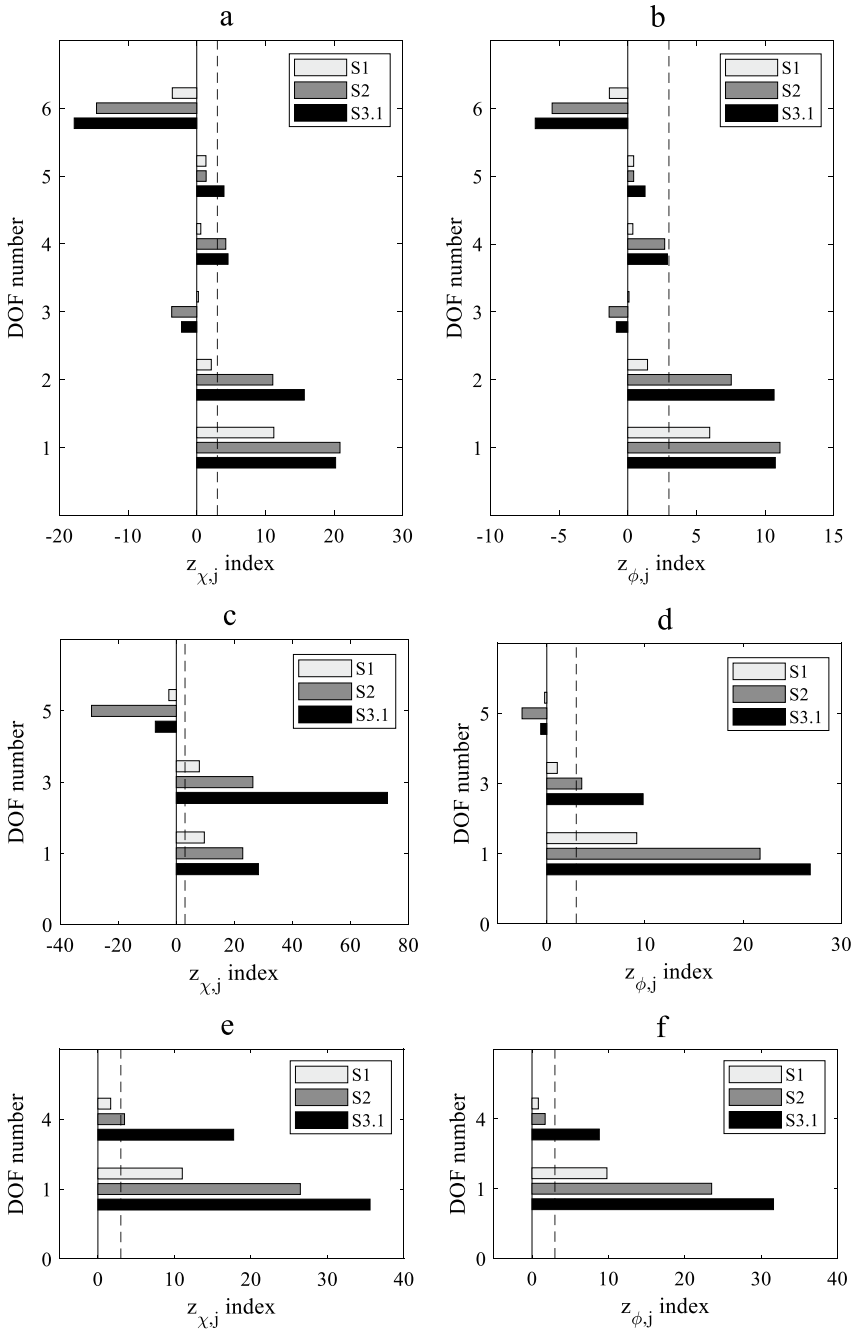


**Fig. 4** Damage detection and localization for the structure in the different states. Approaches: **a**, **c**, **e** z index based on curvature; **b**, **d**, **f** z index based on damage-induced rotation. Scenarios: **a**, **b** 7 measured DOFs; **c**, **d** 4 measured DOFs; **e**, **f** 3 measured DOFs

based on damage-induced rotation. As shown in Fig. 4b, d and f for all three considered scenarios with a different number of measured DOFs, the values of the z index tend to decrease from the upper to the lower DOFs and the maximum value of the z index is at the DOF number 1. This trend is consistent with the concentration of damage at the bottom of the structure observed in the experimental tests [25].

## 4 Conclusions

In this paper, two approaches for output-only damage detection and localization that are based on the estimation of structural deflections from modal flexibility have been considered and applied. One approach is based on monitoring the curvature of the modal flexibility-based deflections. The other approach is based on tracking eventual variations in the damage-induced rotation along the height of the structure. Such approaches have been applied to the data of a benchmark reinforced concrete shear wall building that was tested on the University of California, San Diego—Network for Earthquake Engineering Simulation (UCSD-NEES) large outdoor unidirectional shake table. In particular, different scenarios characterized by different data sets and by a different number of degrees-of-freedom measured on the structure have been considered in the analyses (i.e., three scenarios with 7, 4, and 3 measured DOFs, respectively). The analyses performed in the different scenarios have demonstrated the applicability of the considered methods on a full-scale structure that has experienced earthquake-induced damage, by providing damage identification results that are consistent with the actual damage observed in the structure, especially for the analyses performed using the second approach based on the estimation of the damage-induced rotations from the modal flexibility-based deflections. This is the main conclusion that can be derived from the analyses performed for the considered case study, and, as potential future developments of the work, it is planned to carry out further investigations and analyses on similar benchmark structures.

**Acknowledgements** The use of the data of the experimental tests performed on the shear wall building using the UCSD-NEES shake table (Englekirk Structural Research Center, San Diego, USA) is gratefully acknowledged.

## References

1. Farrar CR, Worden K (2013) Structural health monitoring: a machine learning perspective, 1st edn. Wiley, Chichester, UK
2. Rainieri C, Fabbrocino G (2014) Operational modal analysis of civil engineering structures. Springer-Verlag, New York
3. Brincker R, Ventura CE (2015) Introduction to operational modal analysis, 1st edn. Wiley, Chichester, UK



4. Rainieri C, Fabbrocino G (2010) Automated output-only dynamic identification of civil engineering structures. *Mech Syst Signal Process* 24(3):678–695
5. Pandey AK, Biswas M (1994) Damage detection in structures using changes in flexibility. *J Sound Vib* 169(1):3–17
6. Bernal D (2001) A subspace approach for the localization of damage in stochastic systems. In: Chang FK (ed) *Structural health monitoring: the demand and challenges, proceedings of the 3rd international workshop in structural health monitoring*, pp 899–908. CRC Press, Boca Raton, FL, USA
7. Gao Y, Spencer BF Jr, Bernal D (2007) Experimental verification of the flexibility-based damage locating vector method. *J Eng Mech* 133(10):1043–1049
8. Duan Z, Yan G, Ou J, Spencer BF (2005) Damage localization in ambient vibration by constructing proportional flexibility matrix. *J Sound Vib* 284:455–466
9. Duan Z, Yan G, Ou J, Spencer BF (2007) Damage detection in ambient vibration using proportional flexibility matrix with incomplete measured DOFs. *Struct Control Health Monit* 14(2):186–196
10. Zhang Z, Aktan AE (1998) Application of modal flexibility and its derivatives in structural identification. *Res Nondestr Eval* 10(1):43–61
11. Koo KY, Sung SH, Park JW, Jung HJ (2010) Damage detection of shear buildings using deflections obtained by modal flexibility. *Smart Mater Struct* 19(11):115026
12. Bernagozzi G, Ventura CE, Allahdadian S, Kaya Y, Landi L, Diotallevi PP (2020) Output-only damage diagnosis for plan-symmetric buildings with asymmetric damage using modal flexibility-based deflections. *Eng Struct* 207:110015
13. Bernagozzi G, Mukhopadhyay S, Betti R, Landi L, Diotallevi PP (2018) Output-only damage detection in buildings using proportional modal flexibility-based deflections in unknown mass scenarios. *Eng Struct* 167:549–566
14. Catbas FN, Gul M, Burkett JL (2008) Damage assessment using flexibility and flexibility-based curvature for structural health monitoring. *Smart Mater Struct* 17(1):015024
15. Koo KY, Lee JJ, Yun CB, Kim JT (2008) Damage detection in beam-like structures using deflections obtained by modal flexibility matrices. *Smart Struct Syst* 4(5):605–628
16. Sung SH, Jung HJ, Jung HY (2013) Damage detection for beam-like structures using the normalized curvature of a uniform load surface. *J Sound Vib* 332(6):1501–1519
17. Sung SH, Koo KY, Jung HJ (2014) Modal flexibility-based damage detection of cantilever beam-type structures using baseline modification. *J Sound Vib* 333(18):4123–4138
18. Catbas FN, Brown DL, Aktan AE (2006) Use of modal flexibility for damage detection and condition assessment: case studies and demonstrations on large structures. *J Struct Eng* 132(11):1699–1712
19. Sung SH, Koo KY, Jung HY, Jung HJ (2012) Damage-induced deflection approach for damage localization and quantification of shear buildings: validation on a full-scale shear building. *Smart Mater Struct* 21(11):115013
20. Le NT, Thambiratnam DP, Nguyen A, Chan THT (2019) A new method for locating and quantifying damage in beams from static deflection changes. *Eng Struct* 180:779–792
21. Quqa S, Landi L, Diotallevi PP (2018) On the use of singular vectors for the flexibility-based damage detection under the assumption of unknown structural masses. *Shock Vibr* 9837694
22. Giordano PF, Limongelli MP (2020) Response-based time-invariant methods for damage localization on a concrete bridge. *Struct Concr* 21(4):1254–1271
23. Restrepo J (2017) Shake table response of full scale reinforced concrete wall building slice (NEES-2006-0203). <https://datacenterhub.org/resources/14548>
24. Panagiotou M, Restrepo JI, Conte JP (2007) Shake table test of a 7 story full scale reinforced concrete structural wall building slice—phase I: rectangular wall section. Report No SSRP-07/07, University of California, San Diego
25. Moaveni B, He X, Conte JP, Restrepo JI (2010) Damage identification study of a seven-story full-scale building slice tested on the UCSD-NEES shake table. *Struct Saf* 32(5):347–356
26. Moaveni B, He X, Conte JP, Restrepo JI, Panagiotou M (2011) System identification study of a 7-story full-scale building slice tested on the UCSD-NEES shake table. *J Struct Eng (ASCE)* 137(6):705–717

27. James GH III, Carne TG, Lauffer JP (1995) The natural excitation technique (NExT) for modal parameter extraction from operating structures. *Int J Anal Exp Modal Anal* 10(4):260–277
28. Juang JN, Pappa RS (1985) An eigensystem realization algorithm for modal parameter identification and model reduction. *J Guid Control Dyn* 8(5):620–627